Intermolecular interaction effects on the second hyperpolarizability of open-shell singlet diphenalenyl radical dimer

ARTICLE *in* CHEMICAL PHYSICS LETTERS · MARCH 2008

Impact Factor: 1.9 · DOI: 10.1016/j.cplett.2008.01.084

Available online at www.sciencedirect.com
ScienceDirect
Chemical Physics Letters 454 (2008) 97–104
CHEMICAL PHYSICS LETTERS
www.elsevier.com/locate/cplett

Intermolecular interaction effects on the second hyperpolarizability of open-shell singlet diphenalenyl radical dimer

Masayoshi Nakano [a,*], Akihito Takebe [a], Ryohei Kishi [a], Hitoshi Fukui [a], Takuya Minami [a], Kazuki Kubota [a], Hideaki Takahashi [a], Takashi Kubo [b], Kenji Kamada [c], Koji Ohta [c], Benoît Champagne [d], Edith Botek [d]

[a] Department of Materials Engineering Science, Graduate School of Engineering Science, Osaka University, Toyonaka, Osaka 560-8531, Japan
[b] Department of Chemistry, Graduate School of Science, Osaka University, Toyonaka, Osaka 560-0043, Japan
[c] Photonics Research Institute, National Institute of Advanced Industrial Science and Technology (AIST), Ikeda, Osaka 563-8577, Japan
[d] Laboratoire de Chimie Théorique Appliquée, Facultés Universitaires Notre-Dame de la Paix (FUNDP), rue de Bruxelles, 61, 5000 Namur, Belgium

Received 9 December 2007; in final form 28 January 2008
Available online 5 February 2008

Abstract

We investigate the longitudinal static second hyperpolarizability (γ) of open-shell singlet diphenalenyl radical dimer using the spin-unrestricted density functional theory method. This dimer is known to be a model unit of a slipped stacked linear chain with an unusually short average π–π distance of 3.137 Å. The longitudinal γ per monomer for this dimer is found to be significantly (about twice) enhanced as compared to that of monomer. This originates in the field-induced intermolecular virtual charge transfer between both-end phenalenyl rings through the strong covalent interaction between the unpaired electrons of the cofacial phenalenyl rings.

1. Introduction

In a series of papers [1–9], we have recently investigated a new class of nonlinear optical (NLO) systems based on open-shell singlet molecules, and we have evidenced a novel structure–property relationship between the second hyperpolarizability (γ) and the diradical character (y). Indeed, for singlet diradical π-conjugated systems, γ increases with y until it attains a maximum in the intermediate diradical character region, then it decreases. This relationship has been exemplified by ab initio molecular orbital (MO) and density functional theory (DFT) calculations for polycyclic diphenalenyl radicals [2,7], diphenalenyl radicals linked by acetylene conjugated bridge [6], π-conjugated diradical systems involving imidazole rings [3] as well as by two-photon absorption (TPA) measurements on *s*-indaceno[1,2,3-*cd*;5,6,7-*c*′*d*′]diphenalene (IDPL) and dicyclopenta[*b*;*g*]-naphthaleno[1,2,3-*cd*;6,7,8-*c*′*d*′]diphenalene (NDPL) [9]. This behavior has been analyzed using as model the H_2 molecule submitted to dissociation [4] as well as by employing a valence configuration interaction (VCI) scheme [8]. In the latter case, the γ and diradical character are shown to be predictable from feeding the VCI scheme with simple (theoretical or experimental) optical properties. These contributions belong to the recent revival in studying diradicals (also called biradicaloids) and particularly the interplay between their electronic, optical, and magnetic properties [10–17].

In addition, multi-radical linear chains built from diradical monomers have been examined using hydrogen molecular chain models (H_{2n}) presenting different bond lengths and bond length alternations. Specific dependences of γ with chain length, resulting from inter/intra-molecular interaction effects, have been highlighted as compared to their closed-shell analogs [5]. These studies not only have revealed the effects of inter/intra-molecular interactions

* Corresponding author. Fax: +81 668506268.
E-mail address: mnaka@cheng.es.osaka-u.ac.jp (M. Nakano).

0009-2614/$ - see front matter © 2008 Elsevier B.V. All rights reserved.
doi:10.1016/j.cplett.2008.01.084

on the average diradical character, on the longitudinal γ and on their size dependence, but also define guidelines to design open-shell NLO materials.

As an example of real multi-radical systems, Kubo et al. have reported a one-dimensional (1D) chain of IDPLs displaying a slipped stacking arrangement, exhibiting an unusually short π–π distance, large conductivity as well as an absorption peak shifted extraordinarily to the low-energy region [18]. These features are predicted to originate in the resonance structures of intra- and inter-molecular interactions of the unpaired electrons in 1D chain. So far, little is known about the effects of crystal packing on the third-order NLO properties of diradicals. On the other hand, these effects have been investigated for closed-shell systems and particularly for model polyacetylene chains and other carbon species [19–30]. These studies, which addressed the effects of frequency dispersion [19,21,28], of charging [24], of chain length [19–22] as well as of vibrational contributions [23], have evidenced that packing can strongly modify the γ, enhancing it or reducing it as a function of the relative position of the interacting units. Moreover, several investigations have shown that these effects can accurately be reproduced by employing electrostatic interaction schemes, showing that a large part of the effect can be associated with the modifications of the Maxwell field due to the surrounding molecules [20,25,30].

In this Letter, using a hybrid density functional theory (DFT) approach, we therefore investigate the effects of intra- and inter-molecular interactions on the longitudinal γ of IDPL and of its dimer, in relation to their average diradical character. A closed-shell dimer model of PY2 [2], which is a polycyclic hydrocarbon composed of two pyrenes, is also examined to highlight the specificity of open-shell dimers. The present results will contribute to the clarification of unique third-order NLO properties of singlet multi-radical stacked aggregates composed of extended π-conjugated diradical molecules.

2. Methodology

2.1. Model systems and average diradical character

Fig. 1 displays the structures of IDPL and PY2 [2] monomers (a) and of their dimers (b and c). In IDPL and NDPL, which belong to D_{2h} symmetry, the longitudinal axis (z) is defined to be parallel to the main inertial axis, while for PY2 (C_{2h}), the longitudinal axis is along the middle C–C bond (see C1–C3 shown in Fig. 1 in Ref. 2). The IDPL open-shell dimer forms the unit cell of the crystal, which is composed of 1D chains with a slipped stacking arrangement and an average π–π distance of 3.137 Å [18], while the PY2 closed-shell dimer involves cofacial pyrene rings. The geometry of IDPL dimer was determined by the X-ray diffraction data and, for a matter of simplification, its side phenyl rings are replaced by hydrogen atoms. This structure is referred to as model **1** and exhibits slightly asymmetric structures. We also considered a symmetric

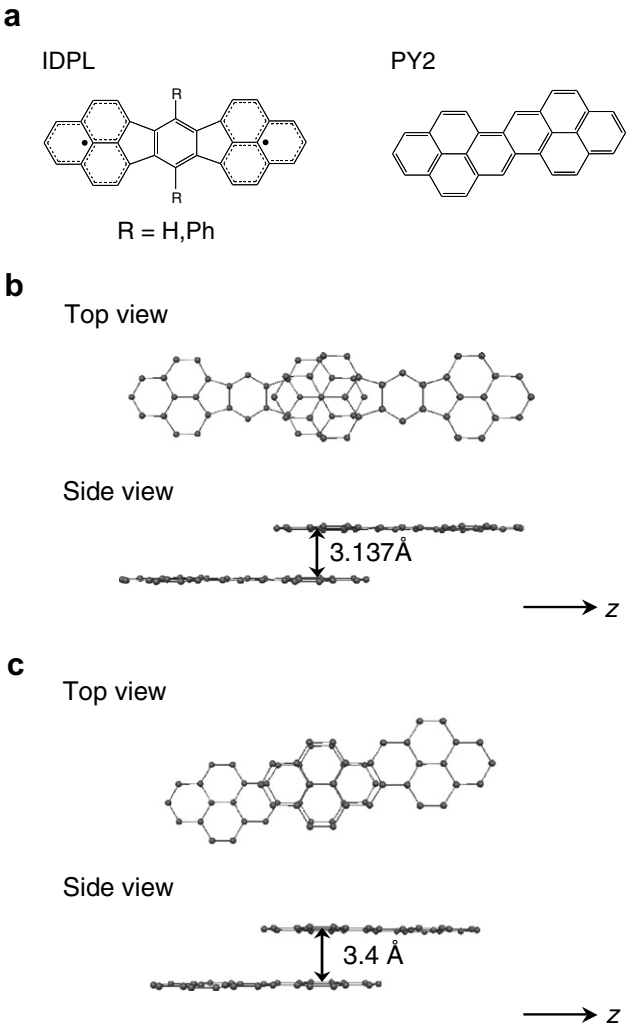

Fig. 1. Structures of IDPL and PY2 monomers (a), IDPL dimer (R = H) (b) extracted from a single crystal (R = Ph) [18] and PY2 dimer (c). The average distance between cofacial phenalenyl rings of IDPL dimer is 3.137 Å, while that of PY2 dimer is fixed to be a typical van der Waals distance 3.4 Å. The structure of PY2 monomer is optimized by the RB3LYP/6-31G** method [2]. The coordinate axis is also shown.

dimer model, which is referred to as model **2**, using the structure of IDPL monomer optimized by the UB3LYP/6-31G** method and the experimental interplanar distance of 3.137 Å. The PY2 dimer model uses the structure of PY2 monomer optimized by the RB3LYP/6-31G** method and a typical van der Waals interplanar distance of 3.4 Å.

The diradical character is obtained from spin-unrestricted Hartree–Fock (UHF) calculations. The diradical character y_i, related to the HOMO $-$ i and LUMO $+$ i, is defined by the weight of the doubly-excited configuration in the multi-configurational (MC)-SCF theory and is formally expressed in the case of the spin-projected UHF (PUHF) theory as [31,32]

$$y_i = 1 - \frac{2T_i}{1 + T_i^2}, \tag{1}$$

where T_i is the orbital overlap between the corresponding orbital pairs [31] ($\chi_{\mathrm{HOMO}-i}$ and $\eta_{\mathrm{HOMO}-i}$) and can also be

represented by using the occupation numbers (n_i) of UHF natural orbitals (UNOs):

$$T_i = \frac{n_{\mathrm{HOMO}-i} - n_{\mathrm{LUMO}+i}}{2}. \quad (2)$$

Since the PUHF diradical characters amount to 0% and 100% for closed-shell and pure diradical states, respectively, y_i represents the diradical character, i.e. the instability of the chemical bond. The present scheme using the UNOs is the simplest but it can well reproduce the diradical characters calculated by other methods such as the ab initio configuration interaction (CI) method [32,33]. In the case of the dimer, we therefore had to consider two pairs of HOMO $- i$ and LUMO $+ i$ ($i = 0$ and 1), which define the diradical characters y_0 and y_1, respectively. The average diradical character (y_{av}) is defined by the arithmetic average of these diradical characters.

2.2. Calculation and analysis methods of γ

The spin restricted (R) and unrestricted (U) BHandHLYP methods [34] are employed to calculate the longitudinal γ (γ_{zzzz}) values of IDPL and PY2 systems, respectively, since previous studies [1–3,6,7] show that they give reliable γ values for closed-shell molecules and diradical molecules with intermediate and large diradical characters. According to our previous studies [1–3,6,7], we use the standard basis set, 6-31G*, which is known to be adequate for semi-quantitative comparisons of, at least, longitudinal components of γ for these large systems. The γ values are calculated using the finite field approach, which consists in the fourth-order differentiation of energy E with respect to different amplitudes of the applied external electric field. Field amplitudes were chosen such as to reduce the numerical accuracy to within 1% of the γ value. All calculations were performed using the GAUSSIAN 03 program package [34].

In order to address the intermolecular interaction-induced effects on γ, we analyzed the γ density, $\rho^{(3)}(\boldsymbol{r})$, determined by numerical differentiation of the electron density $\rho(\boldsymbol{r})$ with respect to the applied field [35]:

$$\rho^{(3)}(\boldsymbol{r}) = \left.\frac{\partial^3 \rho}{\partial F_z \partial F_z \partial F_z}\right|_{\boldsymbol{F}=0}. \quad (3)$$

The relation between γ and its density is given by

$$\gamma = -\frac{1}{3!}\int r_z \rho^{(3)}(\boldsymbol{r})\mathrm{d}\boldsymbol{r}, \quad (4)$$

where r_z denotes the z component of the position vector $\boldsymbol{r}$. The positive and negative values of $\rho^{(3)}(\boldsymbol{r})$ multiplied by F_z^3 represent, respectively, the field-induced increases and decreases in the charge density in proportion to F_z^3. The relationship between γ and $\rho^{(3)}(\boldsymbol{r})$ is explained by considering a simple example: a pair of localized γ densities with positive and negative values. The contribution to γ is positive when the direction from positive to negative γ densities coincides with the (positive) direction of the z axis. Moreover, the magnitude of the contribution associated with this pair of $\rho^{(3)}(\boldsymbol{r})$ is proportional to the distance between them. In order to illuminate the intermolecular interaction effect on γ, we examine the differences of $\rho^{(3)}(\boldsymbol{r})$ between the interacting [$\rho^{(3)}_{\mathrm{int}}(\boldsymbol{r})$] and non-interacting [$\rho^{(3)}_{\mathrm{non\text{-}int}}(\boldsymbol{r})$] systems:

$$\rho^{(3)}_{\mathrm{diff}}(\boldsymbol{r}) = \rho^{(3)}_{\mathrm{int}}(\boldsymbol{r}) - \rho^{(3)}_{\mathrm{non\text{-}int}}(\boldsymbol{r}). \quad (5)$$

3. Results and discussion

3.1. Diradical character, molecular orbital interaction and spin density distribution

Table 1 lists the longitudinal BHandHLYP/6-31G* γ values per monomer (γ/N, N: the number of monomers) of IDPL monomers and dimers [models **1** (using the crystal structure) and **2** (using the optimized monomer structure)] as well as PY2 monomer and dimer models. Because the influence of the basis set superposition error (BSSE) on γ of both dimers is smaller than 1.3% and therefore does not change the semi-quantitative results, we did not use further any procedure for eliminating the BSSE. Although γ(**2**) is slightly larger than γ(**1**), the enhancement is similar as shown by the interaction-induced increase ratio $R = \gamma(\mathrm{dimer})/[2 \times \gamma(\mathrm{monomer})]$, amounting to 1.92 for model **1** vs. 1.99 for model **2**. So, intermolecular interactions lead to a substantial increase of γ for IDPL dimers. It is also noted that such significant increase is specific to the open-shell singlet dimer as seen from the small interaction-induced increase ratio ($R \sim 1.16$) for the analogous PY2 closed-shell neutral dimer ($\gamma/N = 224 \times 10^3$ a.u. for the dimer with an interplanar distance of 3.4 Å vs. 194×10^3 a.u. for the monomer). This specific increase in open-shell singlet dimer is also confirmed by the fact that even another PY2 dimer with the same interplanar distance (3.137 Å) as that of IDPL dimer indicates a smaller interaction-induced increase ratio ($R \sim 1.37$; $\gamma/N = 266 \times 10^3$ a.u. for the dimer with an interplanar distance of 3.137 Å) than IDPL dimer, indicating that most of the enhancement in open-shell singlet dimer is due to the diradical character. In order to reveal the origin of this enhancement, model **2** and PY2 dimer are considered in the following analysis.

Fig. 2a shows the correlation diagram of the frontier orbitals for the monomer and dimer of IDPL obtained at

Table 1
Longitudinal γ (γ_{zzzz}) values [$\times 10^3$ a.u.] per monomer (γ/N, N: the number of monomers) for IDPL monomers and dimers (models **1** and **2**) as well as PY2 monomer and dimer models calculated by the BHandHLYP/6-31G* method[a]

N	Model **1**	Model **2**	PY2
1	2090 (left)[b]	2284	194
	2090 (right)[b]		
2	4003	4539	224

[a] The γ values of IDPL systems are calculated by the UBHandHLYP/6-31G* method, while those of PY2 systems are done by the RBHandHLYP/6-31G* method.

[b] The symbols 'left' and 'right' mean the γ values of left- and right-hand side monomers of the dimer with experimental structure [18].

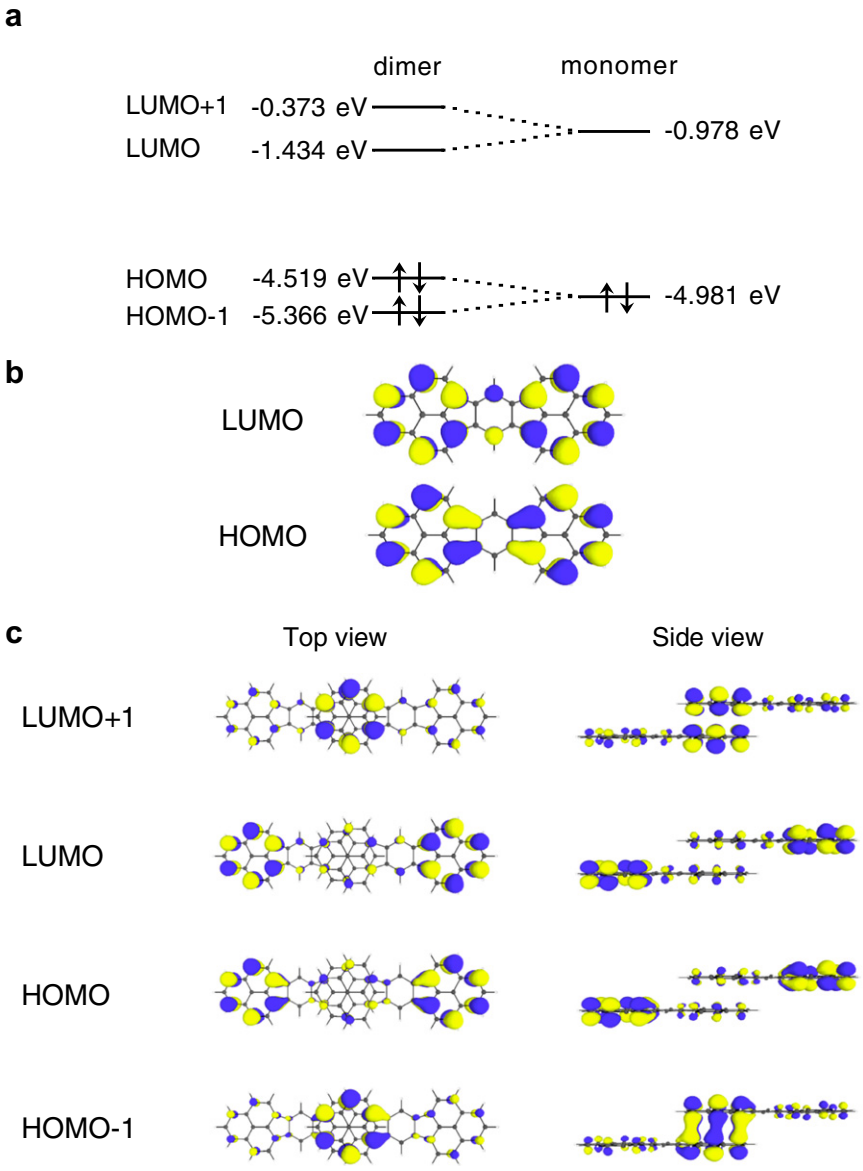

Fig. 2. Correlation diagrams for the RHF frontier orbitals of the monomer and dimer of model **2** (a), spatial distributions of the HOMO and LUMO of UNOs of the monomer (b), as well as of the HOMO − 1, HOMO, LUMO and LUMO + 1 of UNOs of the dimer (c). The yellow and blue surfaces represent positive and negative MOs with iso-surfaces with ±0.025 a.u., respectively. (For interpretation of the references to colour in this figure legend, the reader is referred to the web version of this article.)

the RHF/6-31G* level of approximation. As shown in Ref. [18], the small HOMO–LUMO gap of IDPL (4.003 eV) is caused by the nonbonding character of the frontier orbitals (Fig. 2b), which retain the same character of the singly-occupied molecular orbital (SOMO) of phenalenyl radical. The large spatial overlap between the HOMO and LUMO and the small energy gap lead to the increase of diradical character due to an increase of the weight of the doubly-excited configuration [see Eq. (1)]. As shown in Fig. 2a, the HOMO − 1 and HOMO of the dimer are made from the HOMO–HOMO interactions of two monomers, and a similar reasoning holds for the LUMO's. These interactions lead to a smaller HOMO–LUMO gap (3.085 eV) as well as a larger HOMO − 1 – LUMO + 1 gap (4.993 eV) in the dimer than the HOMO–LUMO gap in the monomer (4.003 eV). These features are expected to cause an increase of y_0 but a decrease of y_1. Indeed, y_0 and y_1 are found to be 0.898 and 0.508, respectively, the average y value (0.703) for dimer being slightly smaller than that of the monomer (0.770). Fig. 2c also shows that HOMO and LUMO of UNOs exhibit dominant distributions at the both-end phenalenyl rings in the dimer, while the HOMO − 1 and LUMO + 1 does dominant distributions at the cofacial phenalenyl rings in the middle region of the dimer. This feature indicates that the primary diradical interaction concerning y_0 occurs between both-end phenalenyl rings in the dimer, whereas that concerning y_1 does between cofacial phenalenyl rings in the middle region of the dimer. This

is consistent with the relative amplitudes of y_0 and y_1: a pair of radicals with larger intersite distance gives larger y values.

As shown in Fig. 3b, the HOMO–LUMO gap of PY2 (7.095 eV) is much larger than that of IDPL (4.003 eV) because of the clear bonding and anti-bonding MOs in the whole region of PY2 in contrast to IDPL. As seen from the correlation diagram for PY2 systems (Fig. 3a), this large HOMO–LUMO gap is also hardly changed (6.569 eV for the dimer), indicating the smaller HOMO–HOMO (LUMO–LUMO) interactions as compared to IDPL systems. This difference between IDPL and PY2 systems also highlights the strong covalent interaction between the unpaired electrons of the cofacial phenalenyl rings in IDPL dimer. Contrary to IDPL dimer, the HOMO and LUMO of PY2 dimer exhibit dominant distribution in the middle region of the dimer, while the HOMO − 1 and LUMO + 1 of the dimer exhibit dominant distribution at the both-end pyrene rings in the dimer (Fig. 3c). This feature and the large HOMO–LUMO gap of the dimer indicates the weak cofacial interaction of PY2 dimer as compared to IDPL dimer.

Mulliken spin density distributions of IDPL monomer (a) and dimer (b) are shown in Fig. 4, in which positive and negative densities represent α and β spin densities, respectively. Because of applying the spin-unrestricted method, symmetry broken spatial distributions of α and β spins are obtained. These can be interpreted to approximately indicate the feature of spatial correlation between α and β spins though these distributions are not observed in real systems. For both the monomer and the dimer, the primary α and β spin density distributions are separated

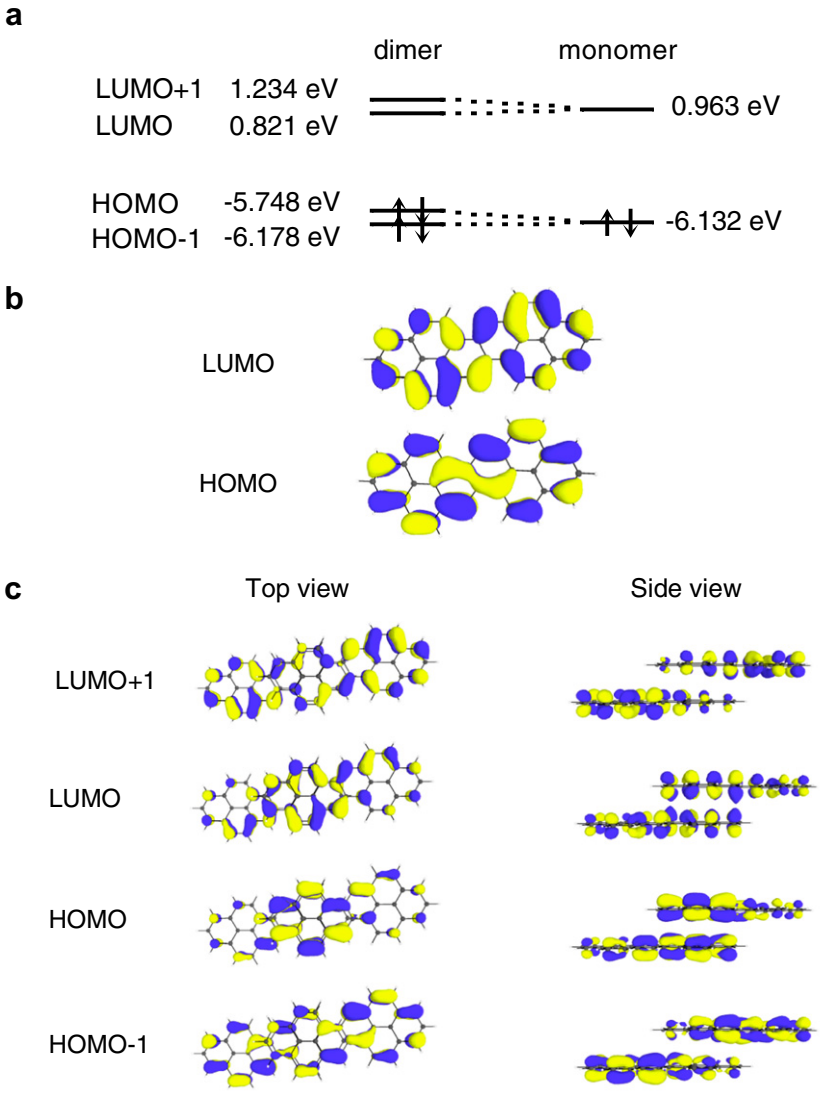

Fig. 3. Correlation diagrams for the RHF/6-31G* frontier orbitals of the monomer and dimer of PY2 (a), spatial distributions of the HOMO and LUMO of the monomer (b), as well as of the HOMO − 1, HOMO, LUMO and LUMO+1 of the dimer (c). The yellow and blue surfaces represent positive and negative MOs with iso-surfaces with ±0.025 a.u., respectively. (For interpretation of the references to colour in this figure legend, the reader is referred to the web version of this article.)

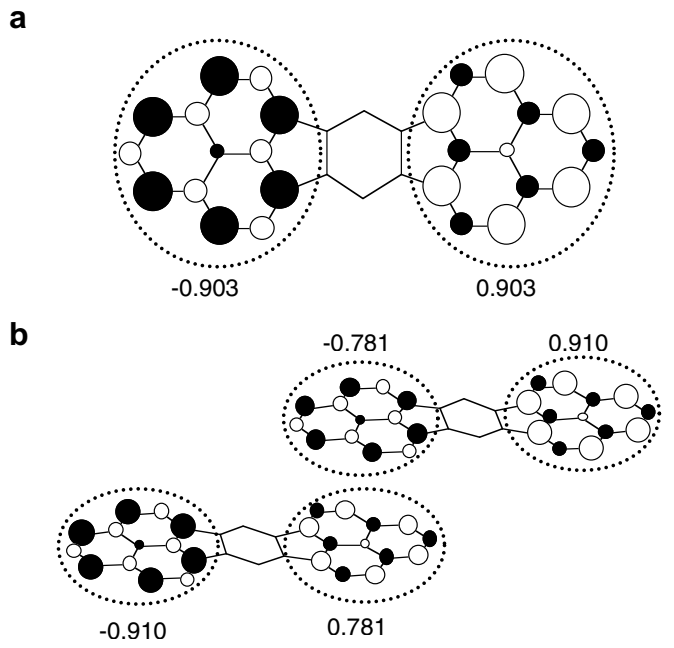

Fig. 4. Mulliken spin densities of IDPL monomer (a) and dimer (b) of model **2** evaluated at the level of UBHandHLYP/6-31G* treatment. The white and black circles represent α and β spin densities, respectively. The values represent the sum of spin densities in the regions surrounded by dotted circles.

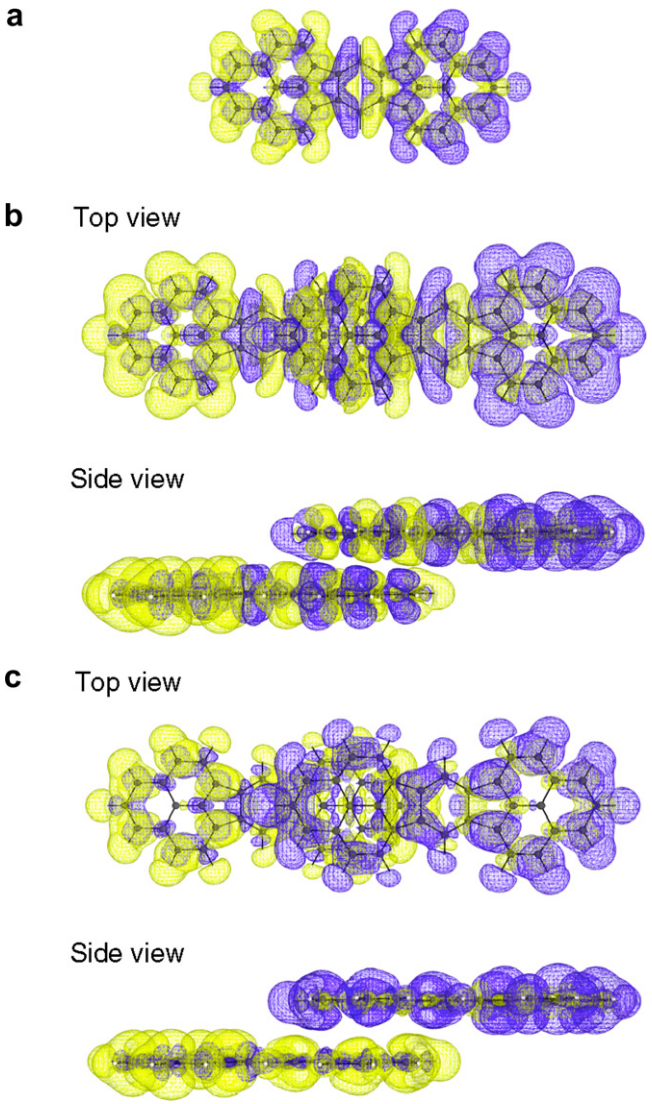

Fig. 5. γ (γ_{zzzz}) density distributions of the monomer (a) and dimer (b) as well as γ density difference [Eq. (5)] for model **2** (c). The yellow and blue meshes represent positive and negative densities with iso-surface $\pm$500 a.u., respectively. (For interpretation of the references to colour in this figure legend, the reader is referred to the web version of this article.)

into right- and left-hand side phenalenyl ring regions, respectively, though spin polarizations are observed in phenalenyl rings. For the dimer case, the spin density distributions on each cofacial phenalenyl ring (0.781) is smaller than that of the monomer (0.903) whereas that of the end-phenalenyl rings (0.910) is larger. These features demonstrate a strong intermolecular covalent interaction and it is agreement with the larger y_0 (0.898) concerning both-end phenalenyl rings in the dimer and the smaller y_1 (0.508) concerning cofacial phenalenyl rings of the dimer than the y_0 (0.770) of the monomer (see Fig. 2c). These alternating spin polarization tend to provide large field-induced fluctuations between intra/inter-phenalenyl rings, leading to a γ enhancement in the dimer as compared to the monomer.

3.2. γ values of dimer

In order to clarify the origin of the significant interaction-induced γ increase in IDPL dimer, we investigated the γ density distributions of the monomer (Fig. 5a) and the dimer (Fig. 5b) as well as γ density difference distributions [Eq. (5)] of the dimer (Fig. 5c). As shown in our previous paper [2], the large γ(monomer) value results from the extended positive and negative π-electron γ densities, which are well-separated on the left- and right-hand side phenalenyl rings, respectively, leading to large positive contribution to γ [Eq. (4)]. This separation is also observed for each monomer building the dimer, while the $\rho^{(3)}(\boldsymbol{r})$ amplitude on the cofacial phenalenyl rings get smaller, leading therefore to positive and negative $\rho^{(3)}(\boldsymbol{r})$ difference on the left and right monomers, respectively. This feature is consistent with the attenuation of the spin polarization between cofacial phenalenyl rings (Fig. 4b) and the decrease in diradical character y_1 as compared to y_0 of the monomer. Namely, the strong covalent interaction (with intermediate diradical character) between the unpaired electrons of the cofacial phenalenyl rings provides a significant interaction-induced increase of γ for the dimer, which is exemplified by the field-induced virtual charge transfer between both-end phenalenyl rings of the dimer. In contrast, as seen from Fig. 6b and c, the closed-shell PY2 dimer (Fig. 6b), the monomer (Fig. 6a) of which gives significantly reduced γ density amplitudes as compared to IDPL [2], exhibits negligible γ density difference distribu-

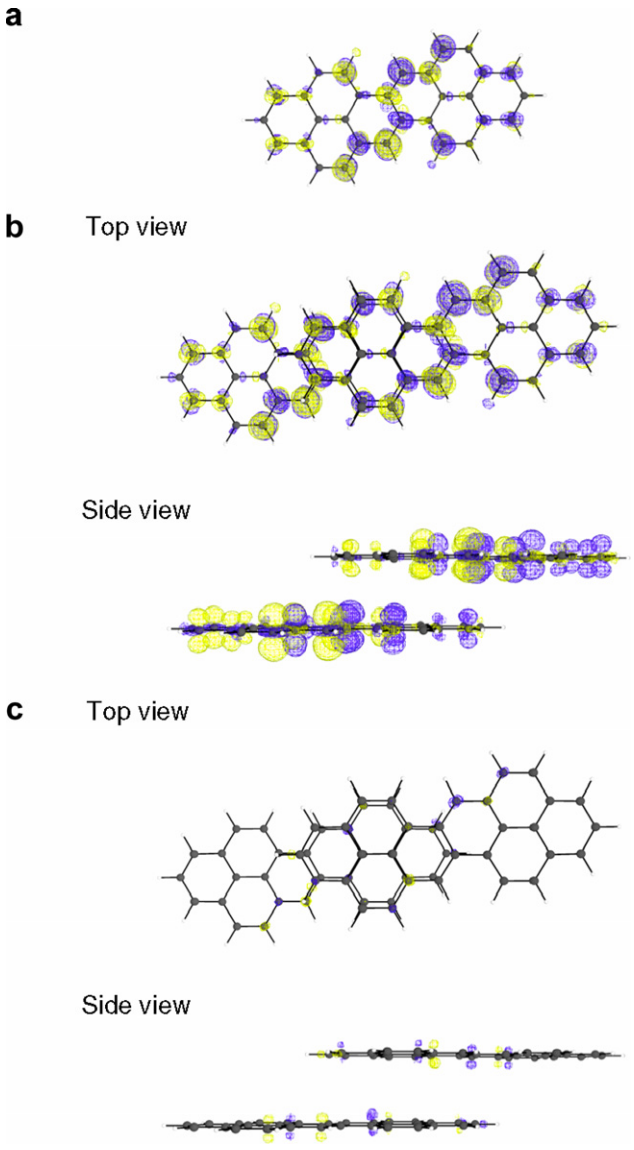

Fig. 6. γ (γ_{zzzz}) density distributions of the monomer (a) and dimer (b) as well as γ density difference [Eq. (5)] for PY2 dimer (c). The yellow and blue meshes represent positive and negative densities with iso-surface $\pm$500 a.u., respectively. (For interpretation of the references to colour in this figure legend, the reader is referred to the web version of this article.)

tions as compared to IDPL dimer. This substantiates the negligible interaction-induced γ values of PY2 dimer.

4. Concluding remarks

Using hybrid DFT approach, we have addressed the impact of intermolecular interactions on the second hyperpolarizability of IDPL by considering a slipped stacked cofacial dimer, which defines IDPL unit cell. This interaction results in a substantial increase of γ per IDPL molecule, in contrast to similar closed-shell neutral species. This effect originates from the strong covalent interaction between the unpaired electrons of cofacial phenalenyl rings, resulting in a small interplanar distance (3.147 Å). The present result also suggests that a remarkable enhancement of γ is expected for open-shell singlet aggregates with intermediate diradical characters when π-delocalization is combined with specific intra- and inter-molecular interactions. This is also in conformity with our previous prediction based on the one-dimensional multi-radical model chains composed of hydrogen molecules [5].

Acknowledgements

This work is supported by Grant-in-Aid for Scientific Research (No. 18350007) from Japan Society for the Promotion of Science (JSPS), Grant-in-Aid for Scientific Research on Priority Areas (No. 18066010) from the Ministry of Education, Science, Sports and Culture of Japan, and the global COE (center of excellence) program 'Global Education and Research Center for Bio-Environmental Chemistry' of Osaka University. E.B. thanks the IUAP Program No. P6-27 for her postdoctoral Grant. B.C. thanks the Belgian National Fund for Scientific Research for his Research Director position.

References

[1] M. Nakano, R. Kishi, et al., J. Phys. Chem. A 109 (2005) 885.
[2] M. Nakano, T. Kubo, et al., Chem. hys. Lett. 418 (2006) 142.
[3] M. Nakano, R. Kishi, et al., J. Phys. Chem. A 110 (2006) 4238.
[4] M. Nakano, R. Kishi, et al., J. Chem. Phys. 125 (2006) 074113.
[5] M. Nakano, A. Takebe, et al., Chem. Phys. Lett. 432 (2006) 473.
[6] S. Ohta, M. Nakano, et al., J. Phys. Chem. A 111 (2007) 3633.
[7] M. Nakano, N. Nakagawa, et al., J. Phys. Chem. A 111 (2007) 9102.
[8] M. Nakano, R. Kishi, et al., Phys. Rev. Lett. 99 (2007) 033001.
[9] K. Kamada, K. Ohta, T. Kubo, et al., Angew. Chem. Int. Ed. 46 (2007) 3544.
[10] D.A. Dougherty, Acc. Chem. Res. 24 (1991) 88.
[11] N. Guihery, D. Maynau, J.P. Malrieu, New J. Chem. 281 (1998).
[12] G. Zoppellaro, A. Geies, V. Enkelmann, M. Baumgarten, Eur. J. Org. Chem. (2004) 2367.
[13] I. Paci et al., J. Am. Chem. Soc. 128 (2006) 16546.
[14] W.W. Porter III, T.P. Vaid, J. Org. Chem. 70 (2005) 5028.
[15] Z. Delen, P.M. Lathi, J. Org. Chem. 71 (2006) 9341.
[16] Md. E. Ali, S.N. Datta, J. Phys. Chem. 110 (2006) 13232.
[17] K. Yesudas, K. Bhanuprakash, J. Phys. Chem. A 111 (2007) 1943.
[18] T. Kubo, A. Shimizu, et al., Angew. Chem. Int. Ed. 44 (2005) 6564.
[19] P.C.M. McWilliams, Z.G. Soos, J. Chem. Phys. 95 (1991) 2127.
[20] B. Kirtman, in: S.P. Karna, A.T. Yeates (Eds.), Theoretical and Computational Modeling of NLO and Electronic Materials, American Chemical Society Series, Vol. 628, American Chemical Society, D.C., New York, 1996, p. 58.
[21] S.Y. Chen, H.A. Kurtz, Structure 388 (1996) 79.
[22] T. Hamada, Faraday Trans. 92 (1996) 3165.
[23] B. Champagne, B. Kirtman, J.Phys. 109 (1998) 6450.
[24] O. Xie, C.W. Dirk, J. Phys. Chem. B 102 (1998) 9378.
[25] B. Kirtman, C.E. Dykstra, B. Champagne, Chem. Phys. Lett. 305 (1999) 132.
[26] L. Jensen, P.O. Åstrand, A. Osted, J. Kongsted, K.V. Mikkelsen, J. Chem. Phys. 116 (2002) 4001.
[27] L. Jensen, K.O. Sylvester-Hvid, K.V. Mikkelsen, P.O. Åstrand, J. Phys. Chem. A 107 (2003) 2270.
[28] E. Botek, B. Champagne, Chem. Phys. Lett. 370 (2003) 197.
[29] M. Nakano, R. Kishi, T. Nitta, B. Champagne, E. Botek, K. Yamaguchi, Int. J. Quantum Chem. 102 (2005) 702.

[30] M. Guillaume, B. Champagne, Phys. Chem. Chem. Phys. 7 (2005) 3284.
[31] K. Yamaguchi, in: R. Carbo, M. Klobukowski (Eds.), Self-Consistent Field: Theory and Applications, Elsevier, Amsterdam, 1990, p. 727.
[32] S. Yamanaka, M. Okumura, M. Nakano, K. Yamaguchi, J. Mol. Structure 310 (1994) 205.
[33] D. Herebian, K.E. Wieghardt, F. Neese, J. Am. Chem. Soc. 125 (2003) 10997.
[34] M.J. Frisch et al., GAUSSIAN 03, Revision B.04, Gaussian Inc., Pittsburgh, PA, 2003.
[35] M. Nakano, I. Shigemoto, S. Yamada, K. Yamaguchi, J. Chem. Phys. 103 (1995) 4175.